PHYSICAL REVIEW A VOLUME 29, NUMBER 4 APRIL 1984

Origin of spectral holes in pump-probe studies of homogeneously broadened lines

Robert W. Boyd
The Institute of Optics, University of Rochester, Rochester, New York 14627

Shaul Mukamel
Department of Chemistry, University of Rochester, Rochester, New York 14627
(Received 31 May 1983)

The theory of pump-probe experiments is examined using the nonlinear optical susceptibility $\chi^{(3)}$. The results of this calculation are shown to differ from those based on a commonly employed heuristic model of pump-probe experiments which assumes that the pump beam "prepares" the system which the probe beam subsequently monitors. This model consequently accounts only for processes where the interactions with the pump field come first in time. The correct expression for the probe absorption line shape as predicted by $\mathrm{Im}\chi^{(3)}$ contains a sum over all the possible time orderings of the various radiative interactions. The interference terms missing from the simplified treatment are shown to account for the spectral hole in homogeneously broadened lines observed recently [L. W. Hillman *et al.*, Opt. Commun. 45, 416 (1983)]. In addition we derive a generalized expression for $\chi^{(3)}$ that is valid away from the impact limit and contains a realistic population relaxation (T_1) matrix.

I. INTRODUCTION

Pump-probe experiments are a standard technique of nonlinear optics used to determine how the optical properties of a medium are modified by a strong pump beam. Such experiments are often interpreted by assuming that the pump beam "prepares" the system which the weak, nonsaturating probe beam subsequently monitors.[1] For reasons that will be clarified in the following paragraph, we shall refer to this approach as the "sequential" interpretation of pump-probe experiments. In accordance with this interpretation, the attenuation experienced by the probe beam is determined by first calculating the equilibrium steady state created by the pump field and then calculating the response of the perturbed system to the probe. A classic application of this approach is given by spectral hole-burning experiments in inhomogeneously broadened absorption lines. In such experiments, the pump beam saturates one segment of the inhomogeneous absorption profile (e.g., one velocity group for the case of Doppler broadening), and hence the probe beam experiences decreased absorption when its frequency is near that of the saturating pump beam.[1] The sequential approach further implies that for a homogeneously broadened system in the presence of a saturating pump, the probe absorption profile will decrease uniformly and cannot have such a hole. However, several theoretical treatments[2–4] and the results of a recent experiment[5] are in marked contrast with this prediction. Schwartz and Tan[2] have shown that it is possible to produce such a hole even in the case of a homogeneously broadened absorption line. A number of more recent papers[3,4] have attributed the origin of this hole to "population oscillations," i.e., the periodic modulation of the ground-state population at the beat frequency between the pump and probe beams. In a recent experiment, Hillman *et al.*[5] have observed such a hole in the green absorption band of ruby and have ascribed the origin of this feature to the mechanism described above.

Some confusion still surrounds this issue, in part because it is not clear exactly where the seemingly plausible sequential treatment of pump-probe experiments breaks down. The intent of this paper is to present a systematic treatment of pump-probe experiments that shows where this breakdown occurs. We show that the failure arises from the artificial decomposition of the applied field into "pump" and "probe" parts which are treated differently by the sequential formalism. In contrast, our calculation is based on an application of the nonlinear susceptibility commonly used to describe coherent, nonlinear optical processes.[6] In this formalism the pump and probe fields are naturally treated in a symmetrical way. We show that the nonlinear susceptibility contains contributions corresponding to all possible time orderings of the interactions with the two applied fields. Conversely, the sequential treatment of pump-probe experiments contains only contributions in which the pump field acts first and only later does the probe field interact with the system. This prescription may be valid for certain experiments involving the sequential application of a pulsed laser beam, but is fundamentally wrong when both fields act simultaneously, as in experiments using cw lasers. In fact, the constraint that the pump act first violates the principles of elementary perturbation theory which require that all time orderings be taken into account. We further show that it is precisely those terms which are omitted in the sequential treatment that correspond to the interference between the two fields and give rise to the hole in the probe absorption profile.

The main results of this paper are as follows. (1) We derive an expression for the nonlinear susceptibility $\chi^{(3)}$

which generalizes that of Bloembergen *et al.*[7] in two respects. (a) We incorporate a more realistic population relaxation (T_1) matrix which describes the relaxation of population among the interacting levels. The famous 48-term expression of Bloembergen *et al.* assumes a diagonal population relaxation (T_1) matrix, and hence can treat only the relaxation of population out of the interacting levels. (b) Our expression is not limited to the impact limit of line broadening, and therefore is valid even at large detunings.[8,9] (2) We relate our expression for $\chi^{(3)}$ to standard diagramatic techniques (i.e., double-sided Feynman diagrams[10,11]) in order to display graphically the terms omitted by the conventional treatments.[1] (3) We show that a spectral hole in a homogeneously broadened line is predicted even in the limit of third-order perturbation theory, and hence that it is not necessary to treat the interaction to all orders in the pump amplitude, as was done in previous treatments.[2-4] Furthermore, we show explicitly that a dip is predicted both for two-level systems and for systems that relax nonradiatively via one or more intermediate levels.

II. $\chi^{(3)}$ FOR A SYSTEM WITH A REALISTIC POPULATION RELAXATION (T_1) MATRIX

Our calculation of the probe absorption line shape will be based on a standard application of the nonlinear $\chi^{(3)}$ susceptibility (Fig. 1).[6] To that end we could have used the 48-term expression for $\chi^{(3)}$ as derived by Bloembergen *et al.*[7] However, in that expression the effects of population relaxation (T_1 processes) are incorporated merely by the addition of an imaginary part to the energies of the various levels. This procedure takes care only of the finite lifetimes of the individual levels. A more realistic description of T_1 processes should include also the effects of transfer of population among the various levels. This may properly be accomplished by the introduction of a T_1 *relaxation matrix* whose diagonal elements are the inverse lifetimes of the levels and whose off-diagonal elements represent the population transfer rates. This relaxation matrix guarantees the conservation of probability and eliminates some unphysical aspects of the conventional expression[7] (i.e., the divergence of $\chi^{(3)}$ that occurs whenever one of the levels has an infinite lifetime). In this section we shall therefore derive a more complete expression for $\chi^{(3)}$ for a system consisting of two radiatively coupled levels and an arbitrary number of levels which participate in the relaxation process. Moreover, our expression, which is based on the factorization approximation developed recently for general multiphoton processes,[8,9,12] is not restricted to the impact limit and allows the inclusion of any single-photon line-shape function in the calculation of $\chi^{(3)}$.

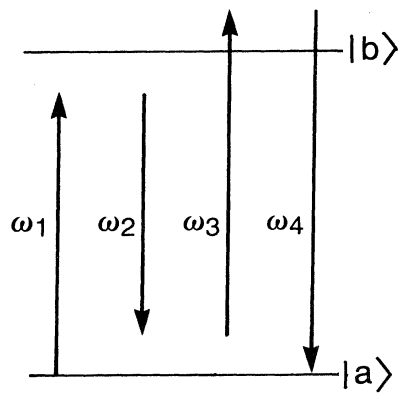

FIG. 1. Energy-level diagram and optical frequencies used in the calculation of the $\chi^{(3)}$ susceptibility for a two-level system.

We consider a system driven by a time-dependent classical field. The Hamiltonian for the perturbed system is given by

$$H = H_0 + \tilde{V}(t) , \tag{1}$$

where H_0 denotes the unperturbed (field-free) Hamiltonian and where $\tilde{V}(t)$ denotes the perturbation, which is due to the superposition of three externally applied monochromatic fields

$$\tilde{V}(t) = V[E_1 \exp(-i\omega_1 t) + E_2 \exp(-i\omega_2 t) + E_3 \exp(-i\omega_3 t)] + \text{c.c.} \tag{2}$$

Here, E_j is the amplitude of the jth field and V is the dipole operator of the material system, and $\tilde{\mathscr{V}} \equiv [V, \cdots]$ is its tetradic analog. The Liouville equation for the density matrix ρ is

$$\frac{d\rho}{dt} = -iL\rho = -i[L_0 + \tilde{\mathscr{V}}(t)]\rho , \tag{3}$$

where

$$L \equiv [H, \cdots] , \tag{4a}$$

$$L_0 \equiv [H_0, \cdots] , \tag{4b}$$

and

$$\tilde{\mathscr{V}}(t) \equiv [\tilde{V}(t), \cdots] \tag{4c}$$

are Liouville-space (tetradic) operators. The definition (4b) implies that $L_0 A \equiv [H_0, A]$ for any operator A, etc.

Assuming that at time $t \to -\infty$, $\rho(-\infty)$ is an equilibrium distribution of H_0, i.e.,

$$L_0 \rho(-\infty) = 0 , \tag{5}$$

we may write the formal expression for the time-dependent density matrix $\rho(t)$ as follows:

$$\rho(t) = U(t, -\infty)\rho(-\infty) \equiv \rho^{(0)} + \rho^{(1)} + \rho^{(2)} + \cdots . \tag{6}$$

Here, U is the propagator

$$U(t,-\infty)=1-i\int_{-\infty}^{t}d\tau\, G_0(t-\tau)\tilde{\mathscr{V}}(\tau)+(-i)^2\int_{-\infty}^{t}d\tau_1\int_{-\infty}^{\tau_1}d\tau_2 G_0(t-\tau_1)\tilde{\mathscr{V}}(\tau_1)G_0(\tau_1-\tau_2)\tilde{\mathscr{V}}(\tau_2)+\cdots\ , \tag{7}$$

where

$$G_0(\tau)=\exp(-iL_0\tau) \tag{8}$$

and $\rho^{(j)}$ is the term in the expansion [Eq. (6)] that is of jth order in $\tilde{\mathscr{V}}$.

The nonlinear polarization $P(\omega_4)$ is related to the expectation value of the dipole operator V at steady state which oscillates at frequency $\omega_4\equiv\omega_1-\omega_2+\omega_3$ through[6]

$$P(\omega_4)\equiv N\,\mathrm{Tr}[V\rho(t)]\equiv\chi^{(3)}(-\omega_4,\omega_1,-\omega_2,\omega_3)E_1E_2^*E_3\exp(-i\omega_1 t+i\omega_2 t-i\omega_3 t)\ , \tag{9}$$

where $\chi^{(3)}$ is the nonlinear susceptibility for a collection of N absorbers per unit volume evaluated to third order in $\mathscr{V}$. We thus have[9]:

$$\chi^{(3)}(-\omega_4,\omega_1,-\omega_2,\omega_3)=N\sum_{\hat{P}(\omega_1,-\omega_2,\omega_3)}\sum_{a}\langle\langle V\mid G_0(\omega_1-\omega_2+\omega_3)\mathscr{V}G_0(\omega_1-\omega_2)\mathscr{V}G_0(\omega_1)\mathscr{V}\mid a,a\rangle\rangle\bar{P}(a)\ , \tag{10}$$

where

$$G_0(\omega)\equiv\frac{1}{\omega-L_0+i\epsilon}\ , \tag{11}$$

and where the limit $\epsilon\to 0$ is to be taken at the end of the calculation. We have further taken

$$\rho(-\infty)=\sum_a\bar{P}_a\mid a,a\rangle\rangle\ , \tag{12}$$

where $\bar{P}_a$ is the population of level $\mid a\rangle$ at thermal equilibrium, in the absence of any radiation field. The $\hat{P}(\omega_1,-\omega_2,\omega_3)$ summation implies that we should sum over all six permutations of the three fields. It is advantageous to transform Eq. (10) to the time domain in order to display explicitly the time ordering of the various interactions. To this end we split L_0 into a system part (L_s) and a bath part (L'). The system part consists of a four-level system with a phenomenological T_1 relaxation matrix $\vec{\Gamma}$ describing the relaxation of the populations to thermal equilibrium in the absence of driving. We thus have

$$L_0\equiv L_s+L'\ , \tag{13}$$

where

$$L_s\equiv[H_s,\cdots]+\vec{\Gamma}\ , \tag{14a}$$

$$L'\equiv[H',\cdots]\ , \tag{14b}$$

$$H_s\equiv\sum_\nu\mid\nu\rangle\epsilon_\nu\langle\nu\mid\ , \tag{15a}$$

$$H'\equiv\sum_\nu\mid\nu\rangle F_\nu(Q_B)\langle\nu\mid\ . \tag{15b}$$

Here $\mid\nu\rangle=\mid a\rangle,\mid b\rangle,\mid c\rangle$, etc. denotes the states of the system with energies ϵ_ν, Q_B are the bath degrees of freedom, and F_ν is the bath Hamiltonian which depends on the state of the system. Furthermore, $\underline{\Gamma}$ is the T_1 relaxation matrix defined by

$$\left[\frac{d}{dt}\rho_{\mu\nu}\right]_{\text{relaxation}}=\sum_{\nu',\mu'}\langle\langle\nu,\mu\mid\underline{\Gamma}\mid\nu',\mu'\rangle\rangle\rho_{\nu'\mu'}\ . \tag{16}$$

The elements of $\vec{\Gamma}$ are defined as follows. (i) The decay rate $\gamma_{\mu\nu}$ of level ν to level μ defines the off-diagonal elements of $\vec{\Gamma}$:

$$\langle\langle\mu,\mu\mid\vec{\Gamma}\mid\nu,\nu\rangle\rangle\equiv\gamma_{\mu\nu},\quad\nu\neq\mu\ . \tag{17a}$$

These terms have been ignored in previous calculations[7] of $\chi^{(3)}$. (ii) The total decay rate of level ν is given by

$$\langle\langle\nu,\nu\mid\vec{\Gamma}\mid\nu,\nu\rangle\rangle\equiv-\gamma_\nu=-\sum_{\mu\,(\neq\nu)}\langle\langle\mu,\mu\mid\vec{\Gamma}\mid\nu,\nu\rangle\rangle. \tag{17b}$$

The second equality is a necessary and sufficient condition to guarantee the conservation of probability in Master equations.[13] (iii) The damping rates of the off-diagonal density-matrix elements due to T_1 processes are given by

$$\langle\langle\nu,\mu\mid\vec{\Gamma}\mid\nu,\mu\rangle\rangle\equiv\tfrac{1}{2}(\gamma_\nu+\gamma_\mu),\quad\nu\neq\mu\ . \tag{17c}$$

(iv) All other elements of $\vec{\Gamma}$ are zero. Using these definitions we may write[9]:

$$\chi^{(3)}(-\omega_4,\omega_1,-\omega_2,\omega_3)$$
$$=(-i)^3N\sum_{\hat{P}(\omega_1,-\omega_2,\omega_3)}\sum_a\int_0^\infty d\tau_1\int_0^{\tau_1}d\tau_3\int_0^{\tau}d\tau_2\exp[i\omega_1\tau_1-i\omega_2(\tau_1-\tau_2)+i\omega_3(\tau_1-\tau_3)]$$
$$\times\langle\langle V(\tau_1)\mid G_s(\tau_1-\tau_3)\mathscr{V}(\tau_3)G_s(\tau_3-\tau_2)\mathscr{V}(\tau_2)G_s(\tau_2)\mathscr{V}(0)\mid a,a\rangle\rangle\bar{P}_a\ , \tag{18}$$

where

$$V(\tau)=\exp(iH'\tau)V\exp(-iH'\tau)\ , \tag{19a}$$

$$\mathscr{V}(\tau)=\exp(iL'\tau)\mathscr{V}\exp(-iL'\tau)\ , \tag{19b}$$

$$G_s(\tau)=\exp(-iL_s\tau)\ , \tag{19c}$$

and

$$G_s(\omega)=\frac{1}{\omega-L_s+i\epsilon}\ . \tag{19d}$$

Equation (18) gives the most general formal expression for the $\chi^{(3)}$ susceptibility. A pictorial representation of Eq. (18) is given in Fig. 2. Each bond (i.e., solid line) denotes a radiative coupling $\mathscr{V}$. The wavy lines that connect $|b,b\rangle\rangle$ to $|a,a\rangle\rangle$ stand for the off-diagonal T_1 relaxation as described by Eq. (17a). Let us first ignore these lines. Since $\mathscr{V}$ is a commutator, it can act either from the right (horizontal lines) or from the left (vertical lines). Figure 2 is an efficient bookkeeping device which keeps track of the eight different three-bond pathways relevant for $\chi^{(3)}$. Each pathway begins at $|a,a\rangle\rangle$ in the upper left-hand corner and the bond which connects it to $|a,b\rangle\rangle$ or $|b,a\rangle\rangle$ represents $\mathscr{V}(0)$ and comes first in time. The second bond in each pathway represents $\mathscr{V}(\tau_2)$ and the third bond represents $\mathscr{V}(\tau_3)$. We note that in the absence of off-diagonal relaxation there will be $2^3=8$ pathways. If we include the wavy lines which represent the process where $|\nu,\nu\rangle\rangle$ relaxes to $|\mu,\mu\rangle\rangle$ via the T_1 processes, then the number of pathways will be doubled and becomes 16. These terms may be combined in groups of four so that we finally get four terms only, resulting in

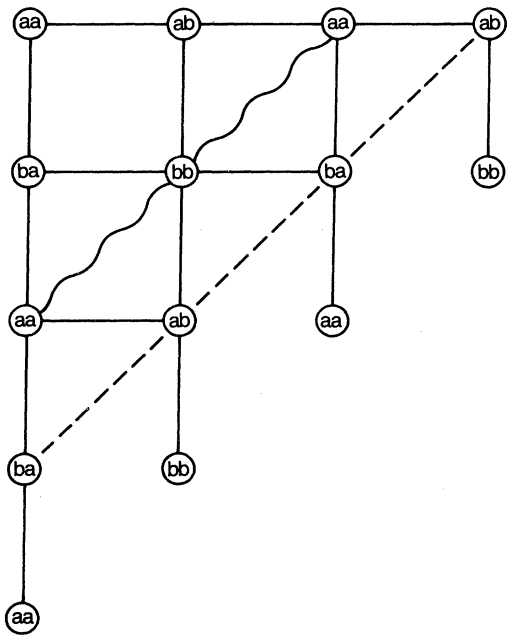

FIG. 2. Pictorial representation (Ref. 9) of the pathways contributing to $\chi^{(3)}$ [Eq. (18)]. The solid lines denote the radiative coupling $\mathscr{V}$. Horizontal (vertical) lines represent action of $\mathscr{V}$ from the right (left). The system starts in the state $|a,a\rangle\rangle$ in the upper left-hand corner and after three perturbations is located along the broken line. The last V acts from the left, and thus at the end of four perturbations the system is in a diagonal state ($|a,a\rangle\rangle$ or $|b,b\rangle\rangle$). The wavy lines connecting $|b,b\rangle\rangle$ to $|a,a\rangle\rangle$ represent the relaxation of population between levels $|a,a\rangle\rangle$ and $|b,b\rangle\rangle$ as given by Eq. (17a). Altogether there are 16 pathways. If we make all six possible permutations of the ω_1, ω_2, and ω_3 fields, there will be $16\times6=96$ terms in the general expression for $\chi^{(3)}$. If we ignore the wavy lines we obtain the $8\times6=48$-term expression of Bloembergen *et al.* (Ref. 7).

$$\chi^{(3)}(-\omega_4,\omega_1,-i\omega_2,\omega_3)\equiv N|\mu_{ba}|^4[\bar{P}(a)-\bar{P}(b)]\hbar^3\sum_{\hat{P}(\omega_1,-\omega_2,\omega_3)}F(-\omega_4,\omega_1,-\omega_2,\omega_3)\ , \tag{20a}$$

where

$$\begin{aligned}F(-\omega_4,\omega_1,-\omega_2,\omega_3)=&-I_{ab}(\omega_1-\omega_2+\omega_3)\hat{I}(\omega_1-\omega_2)I_{ab}(\omega_1)+I_{ba}(\omega_1-\omega_2+\omega_3)\hat{I}(\omega_1-\omega_2)I_{ab}(\omega_1)\\&+I_{ba}(\omega_1-\omega_2+\omega_3)\hat{I}(\omega_1-\omega_2)I_{ba}(\omega_1)-I_{ab}(\omega_1-\omega_2+\omega_3)\hat{I}(\omega_1-\omega_2)I_{ba}(\omega_1)\\=&[I_{ab}(\omega_1)+I_{ba}(\omega_1)]\hat{I}(\omega_1-\omega_2)[I_{ba}(\omega_1-\omega_2+\omega_3)-I_{ab}(\omega_1-\omega_2+\omega_3)]\ .\end{aligned} \tag{20b}$$

The expression for $F(\omega_1,-\omega_2,\omega_3)$ given by Eq. (20b) assumes that the radiative couplings $\mathscr{V}(0)$, $\mathscr{V}(\tau_2)$, and $\mathscr{V}(\tau_3)$ appearing in Eq. (18) are to be associated with the fields ω_1, $-\omega_2$, and ω_3, respectively. Equation (20a) states that to obtain $\chi^{(3)}$ we have to sum over all possible permutations of these three fields, i.e.,

$$\begin{aligned}&\chi^{(3)}(-\omega_4,\omega_1,-\omega_2,\omega_3)\\&\quad\equiv N|\mu_{ba}|^4[\bar{P}(a)-\bar{P}(b)]\hbar^3[F(-\omega_4,\omega_3,-\omega_2,\omega_1)\\&\qquad+F(-\omega_4,\omega_3,\omega_1,-\omega_2)+F(-\omega_4,-\omega_2,\omega_3,\omega_1)\\&\qquad+F(-\omega_4,\omega_1,\omega_3,-\omega_2)+F(-\omega_4,-\omega_2,\omega_1,\omega_3)\\&\qquad+F(-\omega_4,\omega_1,-\omega_2,\omega_3)]\ .\end{aligned} \tag{20c}$$

In Eqs. (20), $\mu_{ba}\equiv\langle b|V|a\rangle$ denotes the electric dipole transition moment connecting levels a and b. The generalized line-shape function $I_{ab}(\omega)$ is defined by[8]

$$\begin{aligned}I_{ab}(\omega)&\equiv\langle\langle a,b|G_0(\omega)|a,b\rangle\rangle\\&=-i\int_0^\infty d\tau\exp(i\omega\tau)\\&\qquad\times\exp[-i\omega_{ab}\tau-\tfrac{1}{2}(\gamma_a+\gamma_b)\tau-g_{ab}(\tau)]\ .\end{aligned} \tag{21}$$

Here, $\omega_{ab}\equiv\epsilon_a-\epsilon_b$ is the frequency of the ab transition, and $g_{ab}(\tau)$ is the line-broadening function which represents the dephasing processes due to the interaction with the bath, and which may be evaluated in numerous

ways.[8] We note that I_{ab} satisfies the Kramers-Kronig relations:

$$I'_{ab}=\frac{-1}{\pi}\mathrm{P}\int_{-\infty}^{\infty}d\omega'\frac{I''_{ab}(\omega')}{\omega'-\omega}\ , \tag{22}$$

where

$$I_{ab}(\omega)\equiv I'_{ab}-iI''_{ab}\ , \tag{23}$$

and I''_{ab} is the ordinary absorption line shape between levels a and b. $I_{ba}(\omega)$ is obtained by interchanging indices in Eq. (23), i.e.,

$$I_{ba}(\omega)=I^{*}_{ab}(-\omega)\ . \tag{24}$$

In the impact limit (short correlation time of the bath), $g_{ab}(\tau)$ is linear in time, i.e.,

$$g_{ab}(\tau)=\hat{\Gamma}_{ab}\,|\,\tau\,|\ , \tag{25a}$$

and substituting into Eq. (21) we get the Lorentzian line shape

$$I_{ab}(\omega)=\frac{1}{\omega-\omega_{ab}+i\Gamma_{ab}}\ , \tag{25b}$$

where

$$\Gamma_{ab}\equiv\tfrac{1}{2}(\gamma_a+\gamma_b)+\hat{\Gamma}_{ab}\ . \tag{25c}$$

Here $\hat{\Gamma}_{ab}$ is the "proper dephasing" contribution to the total line width Γ_{ab}. The $\hat{I}$ term in Eq. (20b) contains the effect of the T_1 relaxation matrix and is given by[8,14]

$$\begin{aligned}\hat{I}(\omega)\equiv&\langle\langle a,a\,|\,G_s(\omega)\,|\,a,a\rangle\rangle+\langle\langle b,b\,|\,G_s(\omega)\,|\,b,b\rangle\rangle\\&-\langle\langle a,a\,|\,G_s(\omega)\,|\,b,b\rangle\rangle-\langle\langle b,b\,|\,G_s(\omega)\,|\,a,a\rangle\rangle\ .\end{aligned} \tag{26}$$

In this paper we consider the three-level relaxation scheme shown in Fig. 3(a). For this model, $\langle\langle b,b\,|\,G_s(\omega)\,|\,a,a\rangle\rangle=0$, and $\hat{I}(\omega)$ can be evaluated using Eqs. (14a), (19b), and (20), resulting in

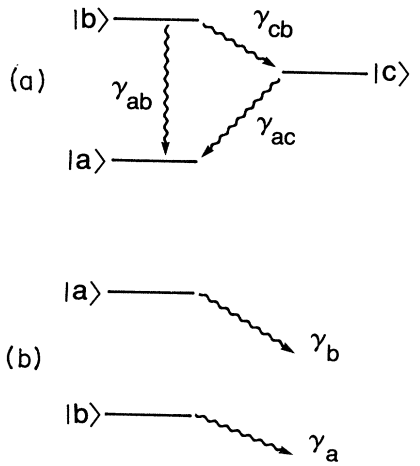

FIG. 3. Models for population relaxation [Eq. (17)]. (a) A three-level system. The inverse-level lifetimes are given by $\gamma_a=0$, $\gamma_b=\gamma_{ab}+\gamma_{cb}$, and $\gamma_c=\gamma_{ac}$ (b) A two-level system without interlevel relaxation as commonly used in the theories of the nonlinear susceptibility (Ref. 7).

$$\hat{I}(\omega)=\frac{2}{\omega+i\gamma_b}+\frac{i\gamma_{cb}}{(\omega+i\gamma_b)(\omega+i\gamma_c)}\ . \tag{27}$$

Equation (20) is a generalization of the expression of Bloembergen *et al.*[7] for $\chi^{(3)}$. This familiar 48-term expression is obtained if we introduce the following two approximations. (i) The impact (Markovian) limit [Eq. (25)]. (ii) We ignore the off-diagonal elements of $\vec{\Gamma}$ [Eq. (17a)] and adopt the simplified relaxation scheme shown in Fig. 3(b). Under these conditions we have

$$\hat{I}(\omega)=\frac{1}{\omega+i\gamma_a}+\frac{1}{\omega+i\gamma_b}\ . \tag{28}$$

$I(\omega)$, given by Eq. (28), diverges whenever $\gamma_a=0$, for instance, when a is the ground state. Equation (27), on the other hand, does not diverge for any physically realizable system.

III. PUMP-PROBE EXPERIMENTS

In this section we apply the results of Sec. II to the calculation of the absorption spectrum experienced by a probe beam of frequency ω_2 in the presence of a pump beam of frequency ω_1. We consider the response of a single atom in a bath to the two applied fields and then multiply by the atomic number density N to obtain the polarization. The polarization $P(\omega_2)$ giving the response at frequency ω_2 is related to the nonlinear susceptibility through

$$\begin{aligned}P(\omega_2)=&\chi^{(1)}(\omega_2)E_2+\chi^{(3)}(-\omega_2,\omega_2,-\omega_1,\omega_1)\,|\,E_1\,|^2E_2\\&+\chi^{(5)}(-\omega_2,\omega_2,-\omega_1,\omega_1-\omega_1,\omega_1)\,|\,E_1\,|^4E_2\\&+\cdots\ .\end{aligned} \tag{29}$$

Since the rate per unit volume at which energy is absorbed from the probe field is proportional to $|\,E_2\,|^2\mathrm{Im}[P(\omega_2)/E_2]$, the absorption coefficient experienced by the probe is given by

$$\begin{aligned}\alpha(\omega_2)\equiv&-\frac{1}{|\,E_2\,|^2}\frac{d}{dz}|\,E_2\,|^2\\=&2\pi\,\mathrm{Im}\chi^{(1)}(\omega_2)\\&+2\pi\,|\,E_1\,|^2\mathrm{Im}\chi^{(3)}(-\omega_2,\omega_2,-\omega_1,\omega_1)+\cdots\ .\end{aligned} \tag{30}$$

We see that $\chi^{(1)}(\omega_2)$ represents the absorption line shape of the E_2 field in the absence of the E_1 field and that $\chi^{(3)}$ represents the correction to the absorption to lowest order in E_1. Hereafter we shall focus on $\chi^{(3)}$ and disregard the higher terms ($\chi^{(5)}$, etc.). We note that, in contrast to Eq. (30), the output signal at frequency $\omega_4=\omega_1-\omega_2+\omega_3$ produced by a coherent four-wave mixing process that is driven by these input fields is proportional to $|\,\chi^{(3)}(-\omega_4,\omega_1,-\omega_2,\omega_3)\,|^2$ rather than $\mathrm{Im}\chi^{(3)}$.

The linear susceptibility $\chi^{(1)}(\omega_2)$ appearing in Eq. (29) is related to the quantity $I_{ab}(\omega_2)$ introduced in the previous section by

$$\chi^{(1)}(\omega_2)=N\,|\,\mu_{ba}\,|^2[\bar{P}(a)-\bar{P}(b)]I_{ab}(\omega_2)/\hbar\ . \tag{31}$$

Making use of Eq. (20b), we obtain an expression for the $\chi^{(3)}$ susceptibility that appears in Eq. (30):

$$\chi^{(3)}(-\omega_2,\omega_2,-\omega_1,\omega_1)=N\,|\,\mu_{ab}\,|^2\{[\bar{P}(a)-\bar{P}(b)]/\hbar^3\}$$
$$\times\{[I_{ba}(\omega_2)-I_{ab}(\omega_2)]\hat{I}(0)[I_{ba}(\omega_1)+I_{ab}(\omega_1)]$$
$$+[I_{ba}(\omega_2)-I_{ab}(\omega_2)]\hat{I}(0)[I_{ba}(-\omega_1)+I_{ab}(-\omega_1)]$$
$$+[I_{ba}(\omega_2)-I_{ab}(\omega_2)]\hat{I}(\omega_1+\omega_2)[I_{ba}(\omega_1)+I_{ab}(\omega_1)]$$
$$+[I_{ba}(\omega_2)-I_{ab}(\omega_2)]\hat{I}(\omega_1+\omega_2)[I_{ba}(\omega_2)+I_{ab}(\omega_2)]$$
$$+[I_{ba}(\omega_2)-I_{ab}(\omega_2)]\hat{I}(\omega_2-\omega_1)[I_{ba}(-\omega_1)+I_{ab}(-\omega_1)]$$
$$+[I_{ba}(\omega_2)-I_{ab}(\omega_2)]\hat{I}(\omega_2-\omega_1)[I_{ba}(\omega_2)+I_{ab}(\omega_2)]\}\ . \tag{32}$$

This general expression for $\chi^{(3)}$ contains, when expanded, $6\times4=24$ terms. For the case of interest in which the fields ω_1 and ω_2 are tuned close to resonance of the ab transition, most of these terms make only a small contribution to the total $\chi^{(3)}$ susceptibility. In the rotating-wave approximation, we ignore any term in Eq. (32) that contains at least one antiresonant $(\omega_1+\omega_2)$ denominator. Thus, only four terms remain:

$$\chi^{(3)}(-\omega_2,\omega_2,-\omega_1,\omega_1)=N\,|\,\mu_{ab}\,|^4\{[\bar{P}(a)-\bar{P}(b)/\hbar^3]\}\{I_{ba}(\omega_2)\hat{I}(0)I_{ba}(\omega_1)+I_{ba}(\omega_2)\hat{I}(0)I_{ab}(-\omega_1)$$
$$+I_{ba}(\omega_2)\hat{I}(\omega_2-\omega_1)I_{ab}(-\omega_1)+I_{ba}(\omega_2)\hat{I}(\omega_2-\omega_1)I_{ba}(\omega_2)\}$$
$$\equiv(\chi^{(3)})_{\rm I},+(\chi^{(3)})_{\rm II}+(\chi^{(3)})_{\rm III}+(\chi^{(3)})_{\rm IV}\ , \tag{33}$$

where $(\chi^{(3)})_{\rm I}$, $(\chi^{(3)})_{\rm II}$, $(\chi^{(3)})_{\rm III}$, and $(\chi^{(3)})_{\rm IV}$ refer to the four contributions to $\chi^{(3)}$ in the order in which they are given in Eq. (33). Since $\hat{I}$ [Eq. (26)] contains four contributions as well, Eq. (33) includes 16 terms corresponding to 16 distinct pathways through the lattice shown in Fig. 2. These pathways are displayed explicitly in Fig. 4.

Let us consider the particular case of the three-level system shown in Fig. 3(a), in which levels a and b are radiatively coupled and level c participates only in the relaxation process. In this case $\hat{I}(\omega)$ is given by Eq. (27) and, assuming the impact limit, $I_{ab}(\omega)$ is given by Eq. (25). Equation (33) for $\chi^{(3)}$ thus becomes

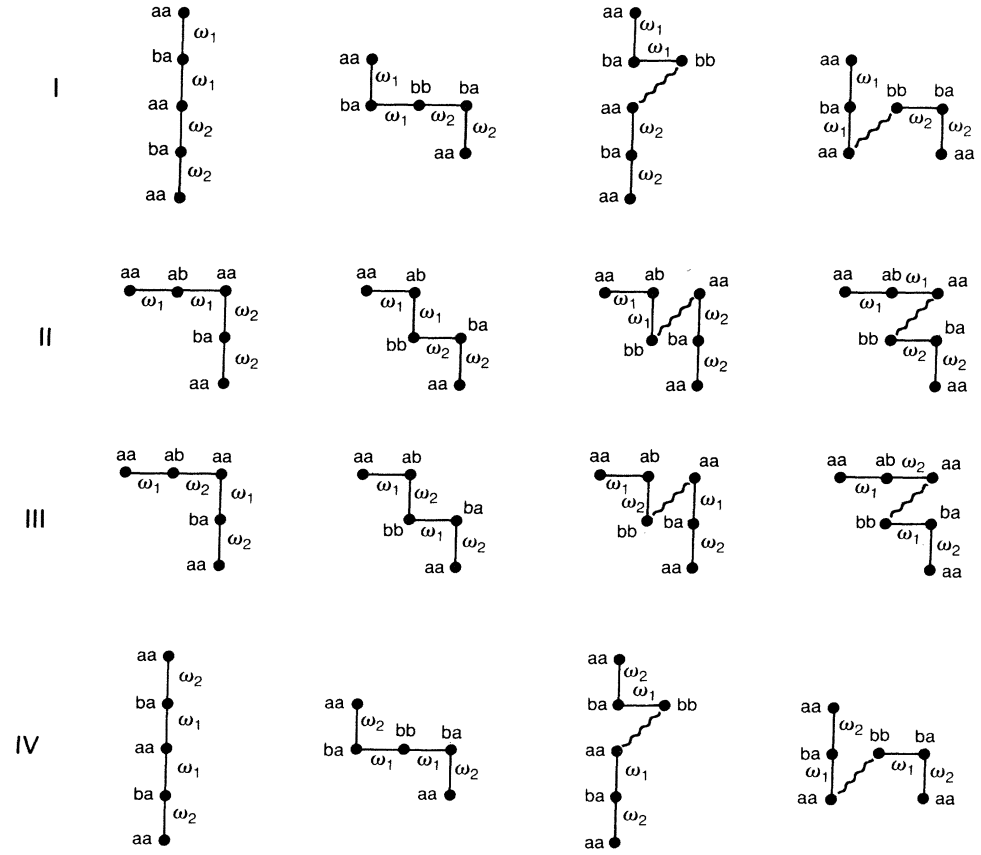

FIG. 4. The 16 pathways contributing to Eq. (33). Row I corresponds to the first term in Eq. (33), and similarly for rows II, III, and IV. Four pathways contribute to each term in Eq. (33), since according to Eq. (26) $\hat{I}$ is itself the sum of four terms.

$$\chi^{(3)}(-\omega_2,\omega_2,-\omega_1,\omega_1)=N\,|\mu_{ba}|^4\{[\bar{P}(a)-\bar{P}(b)]/\hbar^3\}$$

$$\times\left\{\left[\frac{1}{\omega_2-\omega_{ba}+i\Gamma_{ab}}\right]\left[\frac{1}{i\gamma_b}\left[2+\frac{\gamma_{cb}}{\gamma_c}\right]\right]\left[\frac{1}{\omega_1-\omega_{ba}+i\Gamma_{ab}}\right]\right.$$

$$+\left[\frac{1}{\omega_2-\omega_{ba}+i\Gamma_{ab}}\right]\left[\frac{1}{i\gamma_b}\left[2+\frac{\gamma_{cb}}{\gamma_c}\right]\right]\left[\frac{1}{-\omega_1-\omega_{ab}+i\Gamma_{ab}}\right]$$

$$+\left[\frac{1}{\omega_2-\omega_{ba}+i\Gamma_{ab}}\right]\left[\frac{2}{\omega_2-\omega_1+i\gamma_b}+\frac{i\gamma_{cb}}{(\omega_2-\omega_1+i\gamma_b)(\omega_2-\omega_1+i\gamma_c)}\right]\left[\frac{1}{-\omega_1-\omega_{ab}+i\Gamma_{ab}}\right]$$

$$\left.+\left[\frac{1}{\omega_2-\omega_{ba}+i\Gamma_{ab}}\right]\left[\frac{2}{\omega_2-\omega_1+i\gamma_b}+\frac{i\gamma_{cb}}{(\omega_2-\omega_1+i\gamma_b)(\omega_2-\omega_1+i\gamma_c)}\right]\left[\frac{1}{\omega_2-\omega_{ba}+i\Gamma_{ab}}\right]\right\}$$

$$\equiv(\chi^{(3)})_{\rm I}+(\chi^{(3)})_{\rm II}+(\chi^{(3)})_{\rm III}+(\chi^{(3)})_{\rm IV}\,. \tag{34}$$

Upon substitution of Eq. (34) into Eq. (30), we get our final expression for the absorption line shape:

$$\alpha(\omega_2)\equiv\alpha_1(\omega_2)+\alpha_2(\omega_2)\,, \tag{35}$$

where

$$\alpha_1(\omega_2)=2\pi N\,|\mu_{ab}|^2[(\bar{P}_a-\bar{P}_b)/\hbar]\frac{\Gamma_{ab}}{(\omega_{ba}-\omega_2)^2+\Gamma_{ab}^2}\left[1-\frac{4\,|E_1|^2\,|\mu_{ab}|^2}{\hbar^2\gamma_b\Gamma_{ab}}\frac{\Gamma_{ab}^2}{(\omega_1-\omega_{ba})^2+\Gamma_{ab}^2}\right], \tag{35'}$$

$$\alpha_2(\omega_2)=2\pi N\,|\mu_{ab}|^4[(\bar{P}_a-\bar{P}_b)/\hbar^3]$$

$$\times{\rm Im}\left[\left[\frac{1}{\omega_2-\omega_{ba}+i\Gamma_{ab}}\right]\left[\frac{2}{\omega_2-\omega_1+i\gamma_b}+\frac{i\gamma_{cb}}{(\omega_2-\omega_1+i\gamma_b)(\omega_2-\omega_1+i\gamma_c)}\right]\left[\frac{1}{-\omega_1-\omega_{ab}+i\Gamma_{ab}}\right]\right.$$

$$\left.+\left[\frac{1}{\omega_2-\omega_{ba}+i\Gamma_{ab}}\right]\left[\frac{2}{\omega_2-\omega_1+i\gamma_b}+\frac{i\gamma_{cb}}{(\omega_2-\omega_1+i\gamma_b)(\omega_2-\omega_1+i\gamma_c)}\right]\left[\frac{1}{\omega_2-\omega_{ba}+i\Gamma_{ab}}\right]\right]. \tag{35''}$$

Here α_1 comes from the contribution of $\chi^{(1)}$ as well as the $(\chi^{(3)})_{\rm I}$ and $(\chi^{(3)})_{\rm II}$ terms of $\chi^{(3)}$ [Eq. (33)], and α_2 results from the $(\chi^{(3)})_{\rm III}$ and $(\chi^{(3)})_{\rm IV}$ terms of Eq. (33). Equation (35) is our main result for pump-probe experiments. *It should be noted that this equation is in contradiction with the traditional expression for the probe absorption line shape, obtained using the sequential model.* This prescription for the calculation of $\alpha(\omega_2)$ consists of letting the pump "prepare" the system in a nonequilibrium steady state which is then monitored by the probe field. This procedure results in the following expression[1]:

$$\alpha(\omega_2)=2\pi N\,|\mu_{ab}|^2[(\bar{P}_a-\bar{P}_b)_{\rm ss}/\hbar]\frac{\Gamma_{ab}}{(\omega_{ba}-\omega_2)^2+\Gamma_{ab}^2}\,, \tag{36}$$

where $(\bar{P}_a-\bar{P}_b)_{\rm ss}$ is the steady-state value of $\bar{P}_a-\bar{P}_b$ in the presence of the E_1 field only. Substituting the standard steady-state solutions to the Bloch equations in Eq. (36) results in

$$\alpha(\omega_2)=2\pi N\,|\mu_{ab}|^2[(\bar{P}_a-\bar{P}_b)/\hbar]\frac{\Gamma_{ab}}{(\omega_{ba}-\omega_2)^2+\Gamma_{ab}^2}$$

$$\times\frac{(\omega_1-\omega_{ba})^2+\Gamma_{ab}^2}{(\omega_1-\omega_{ba})^2+\Gamma_{ab}^2+\dfrac{4\,|\mu_{ab}|^2\,|E_1|^2}{\hbar^2\gamma_a\Gamma_{ab}}}\,. \tag{37}$$

When Eq. (37) is expanded in $|E_1|^2$ to first order, we obtain only the α_1 term [Eq. (35')]. *The sequential procedure thus fails to account for the second term α_2 [Eq. (35'')] and is therefore incomplete.*

The significance of this omission is clarified by some numerical calculations of Eq. (30), which we now present. In Fig. 5 we display the absorption line shape $\alpha(\omega_2)$ for the case of a pure two-level system (which corresponds to $\gamma_{cb}=0$) in the absence and in the presence of proper dephasing. Figure 5(a) applies to the case of no proper dephasing ($\hat{\Gamma}_{ab}=0$), for example, in a system that is purely radiatively broadened. The upper curve shows the probe absorption profile in the absence of saturation (i.e., $E_1=0$), whereas the lower curve shows the probe absorption profile under conditions whereby the pump beam partially saturates the transition so that the saturation parameter

$$\mathscr{I}\equiv 4\,|\,\mu_{ab}E_1\,|^2/(\hbar^2\Gamma_{ab}\gamma_b) \tag{38}$$

is equal to 0.125. In this limit the probe absorption profile is nearly Lorentzian. In contrast, Fig. 5(b) shows the probe absorption for the case of a transition broadened mainly by dephasing (e.g., collisions) such that $\hat{\Gamma}_{ab}=9.5\gamma_b$ and hence $\Gamma_{ab}=10\gamma_b$. In this case, a pronounced Lorentzian-shaped dip of width $\sim\gamma_b$ centered at the pump-laser frequency is observed. In order to analyze the origin of this spectral feature, we have plotted in Fig. 6 the four contributions to $\mathrm{Im}\chi^{(3)}$ given by the imaginary parts of the terms designated $(\chi^{(3)})_{\mathrm{I}}$, $(\chi^{(3)})_{\mathrm{II}}$, $(\chi^{(3)})_{\mathrm{III}}$, and $(\chi^{(3)})_{\mathrm{IV}}$ in Eq. (34) for each of the cases shown in Fig. 5. Figure 6(a) shows that in the absence of proper dephasing the various terms make similar contributions to the total saturation and that each of the terms has roughly the same line shape. Figure 6(b) shows that in the presence of proper dephasing, the line width associated with the $(\chi^{(3)})_{\mathrm{I}}$ and $(\chi^{(3)})_{\mathrm{II}}$ contributions [$\sim\Gamma_{ab}$ half-width at half maximum (HWHM) in angular frequency units] differs significantly from that of the $(\chi^{(3)})_{\mathrm{III}}$ and $(\chi^{(3)})_{\mathrm{IV}}$ contributions ($\sim\gamma_b$). Hence the imaginary parts of $(\chi^{(3)})_{\mathrm{I}}$ and $(\chi^{(3)})_{\mathrm{II}}$ give rise to the overall saturation of the absorption profile, whereas the imaginary parts of $(\chi^{(3)})_{\mathrm{III}}$ and $(\chi^{(3)})_{\mathrm{IV}}$ give rise to the dip at the pump frequency. *As noted above, the sequential expression [Eq. (37)] contains only contributions $(\chi^{(3)})_{\mathrm{I}}$ and $(\chi^{(3)})_{\mathrm{II}}$ and therefore fails to account for the dip.*

The material system in which this dip was recently observed is ruby.[5] For this case,

$$\gamma_{cb}\gg\gamma_{ab},\gamma_{ac}\ , \tag{39}$$

implying that level b decays predominantly to level c where population is stored before returning to the ground level a. In this limit Eq. (27) reduces to

$$\hat{I}(\omega)=\frac{1}{\omega+i\gamma_c}\ . \tag{40a}$$

On the other hand, for a pure two-level system ($\gamma_{cb}=0$),

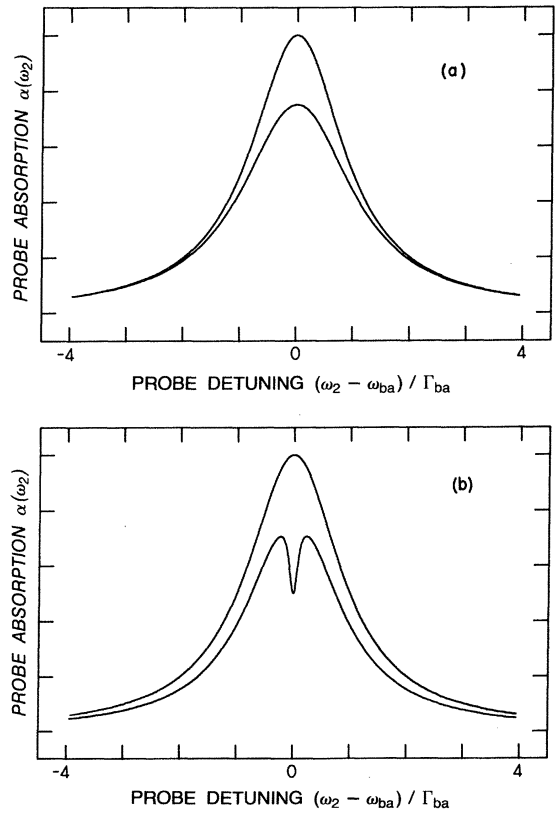

FIG. 5. Probe absorption line shape $\alpha(\omega_2)$ given by Eq. (35) for a two-level system ($\gamma_{cb}=\gamma_a=0$) with the pump laser tuned to line center ($\omega_1=\omega_{ba}$). (a) In the absence of dephasing ($\hat{\Gamma}_{ab}=0$): upper curve, $\mathscr{I}=0$ (no saturation); lower curve, $\mathscr{I}=0.125$ (partial saturation). (b) In the presence of dephasing ($\hat{\Gamma}_{ab}=9.5\gamma_b$): upper curve, $\mathscr{I}=0$ (no saturation); lower curve, $\mathscr{I}=0.25$ (partial saturation).

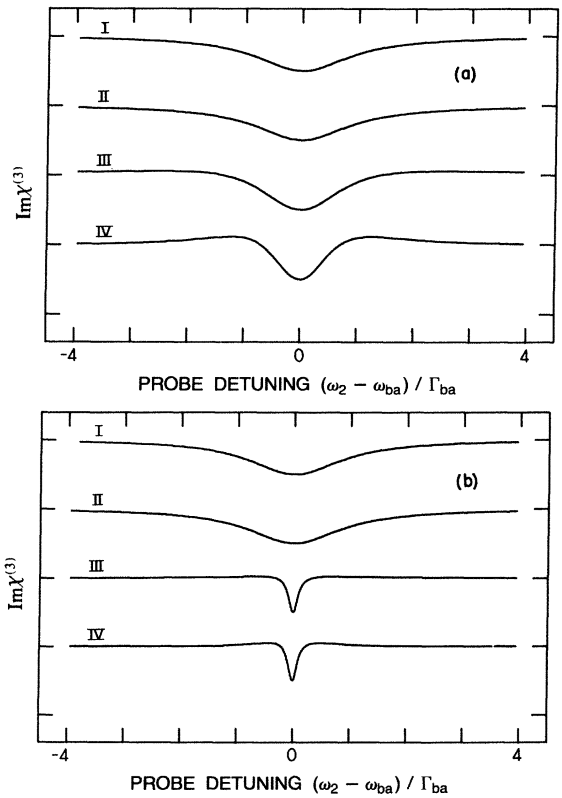

FIG. 6. The four contributions to $\mathrm{Im}\chi^{(3)}$ defined in Eq. (34) (a) in the absence of dephasing ($\hat{\Gamma}_{ab}=0$) [same parameters as Fig. 5(a)] and (b) in the presence of dephasing [same parameters as Fig. 5(b)].

Eq. (27) yields

$$\hat{I}(\omega)=\frac{2}{\omega+i\gamma_b} . \tag{40b}$$

Upon comparing Eqs. (40a) and (40b), we note that the expression for $\chi^{(3)}$ in the limit (39) is equal to one-half of that of a two-level system, provided we replace γ_b by γ_c. Figures 5 and 6 thus also pertain to this case within this factor of 2 and with γ_c replacing γ_b. The two-fold reduction in $\chi^{(3)}$ can be understood as resulting from the absence of stimulated emission effects involving level b due to the rapid decay of this level.

For the values of the decay rates quoted in Ref. 5, Eq. (35) predicts that a Lorentzian-shaped dip of width (half-width at half maximum) ~ 37 Hz will occur at the laser frequency. The predicted line shape is in good agreement with the line shapes measured at low laser power by Hillman *et al.*[5] At higher values of the laser power ($\gtrsim 0.1$ W), significant power broadening of the dip was observed in the experimental study. Higher-order terms in the nonlinear susceptibility ($\chi^{(5)}$, etc.), would have incorporated into the present theory to account for this behavior. It should also be noted that propagation effects were important under the experimental conditions of Hillman *et al.*, and that exact quantitative agreement requires the inclusion of these effects. Such propagation and higher-order nonlinear effects are included in the nonperturbative theory that was found in Ref. 5 to be in good agreement with all of the experimental line shapes.

In order to connect our results with previous works,[10,11] and to give further insight regarding the significance of the $(\chi^{(3)})_{\rm I}$, $(\chi^{(3)})_{\rm II}$, $(\chi^{(3)})_{\rm III}$, and $(\chi^{(3)})_{\rm IV}$ contributions to $\chi^{(3)}$, let us consider the simplified relaxation scheme shown in Fig. 3(b). In this case

$$\hat{I}(\omega)=\frac{1}{\omega+i\gamma_a}+\frac{1}{\omega+i\gamma_b} . \tag{41}$$

Upon the substitution of Eqs. (41) and (25b) into Eq. (33), we get the following expression for $\chi^{(3)}$:

$$\begin{aligned}
\chi^{(3)}(-\omega_2,\omega_2,-\omega_1,\omega_1)=&N|\mu_{ab}|^4\{[\bar{P}(a)-\bar{P}(b)]/\hbar^3\}\\
&\times\left[\left[\frac{1}{(\omega_2-\omega_{ba}+i\Gamma_{ab})(i\gamma_a)(\omega_1-\omega_{ba}-i\Gamma_{ab})}+\frac{1}{(\omega_2-\omega_{ba}+i\Gamma_{ab})(i\gamma_b)(\omega_1-\omega_{ba}-i\Gamma_{ab})}\right]\right.\\
&+\left[\frac{1}{(\omega_2-\omega_{ba}+i\Gamma_{ab})(-i\gamma_a)(\omega_1-\omega_{ba}-i\Gamma_{ab})}+\frac{1}{(\omega_2-\omega_{ba}+i\Gamma_{ab})(-i\gamma_b)(\omega_1-\omega_{ba}-i\Gamma_{ab})}\right]\\
&+\left[\frac{1}{(\omega_2-\omega_{ba}+i\Gamma_{ab})(\omega_2-\omega_1+i\gamma_a)(\omega_1-\omega_{ba}-i\Gamma_{ba})}\right.\\
&\left.+\frac{1}{(\omega_2-\omega_{ba}+i\Gamma_{ab})(\omega_2-\omega_1+i\gamma_b)(\omega_1-\omega_{ba}+i\Gamma_{ab})}\right]\\
&+\left[\frac{1}{(\omega_2-\omega_{ba}+i\Gamma_{ab})(\omega_2-\omega_1+i\gamma_a)(\omega_2-\omega_{ba}+i\Gamma_{ab})}\right.\\
&\left.\left.+\frac{1}{(\omega_2-\omega_{ba}+i\Gamma_{ab})(\omega_2-\omega_1+i\gamma_b)(\omega_2-\omega_{ba}+i\Gamma_{ab})}\right]\right]\\
\equiv&\{[(\chi^{(3)})_{\rm I_a}+(\chi^{(3)})_{\rm I_b}]+[(\chi^{(3)})_{\rm II_a}+(\chi^{(3)})_{\rm II_b}]+[(\chi^{(3)})_{\rm III_a}+(\chi^{(3)})_{\rm III_b}]+[(\chi^{(3)})_{\rm IV_a}+(\chi^{(3)})_{\rm IV_b}]\} .
\end{aligned} \tag{42}$$

This equation can also be obtained from the general 48-term expression of Bloembergen[7] by assuming the following. (1) A two-level system ($a=c$, $b=d$) in the notation of Ref. 7. (2) The particular choice of frequencies relevant to pump-probe experiments. (3) The rotating-wave approximation, which eliminates 40 of the 48 terms. The eight remaining terms come in four pairs corresponding to the $(\chi^{(3)})_{\rm I}$, $(\chi^{(3)})_{\rm II}$, $\chi^{(3)})_{\rm III}$, and $(\chi^{(3)})_{\rm IV}$ contributions of Eq. (33). Note that $(\chi^{(3)})_{\rm I_a}$ [$(\chi^{(3)})_{\rm I_b}$] results from a pathway in Fig. 2 that passes through an internal point $|a,a\rangle\rangle$ ($|b,b\rangle\rangle$) and similarly for terms $(\chi^{(3)})_{\rm II}$, $(\chi^{(3)})_{\rm III}$, and $(\chi^{(3)})_{\rm IV}$. The eight pathways correspond to the first two columns of Fig. 4. Columns 3 and 4 make no contributions for the assumed relaxation scheme [Fig. 3(b)]. Each of the eight terms arises from a distinct pathway in Fig. 2. For the sake of clarity, we display in Fig. 7 each of these eight pathways. In addition, we give the double-sided Feynman diagram corresponding to each pathway.[10,11] It is clearly seen from Fig. 6 that the $({\rm Im}\chi^{(3)})_{\rm I}$ and $({\rm Im}\chi^{(3)})_{\rm II}$ terms arise from pathways in which the two interactions with the E_1 field occur before either of the interactions with the E_2 field. This time ordering enables us to view the process as if the E_1 field "prepares" the system which the E_2 field merely probes. Hence the sequential prescription [Eq. (37)] accounts for these terms $[(\chi^{(3)})_{\rm I_a}+(\chi^{(3)})_{\rm I_b}+(\chi^{(3)})_{\rm II_a}+(\chi^{(3)})_{\rm II_b}]$. However, Fig. 6 shows that in addition we must include those pathways [$(\chi^{(3)})_{\rm III}$ and $(\chi^{(3)})_{\rm IV}$] in which the E_1 and E_2 fields inter-

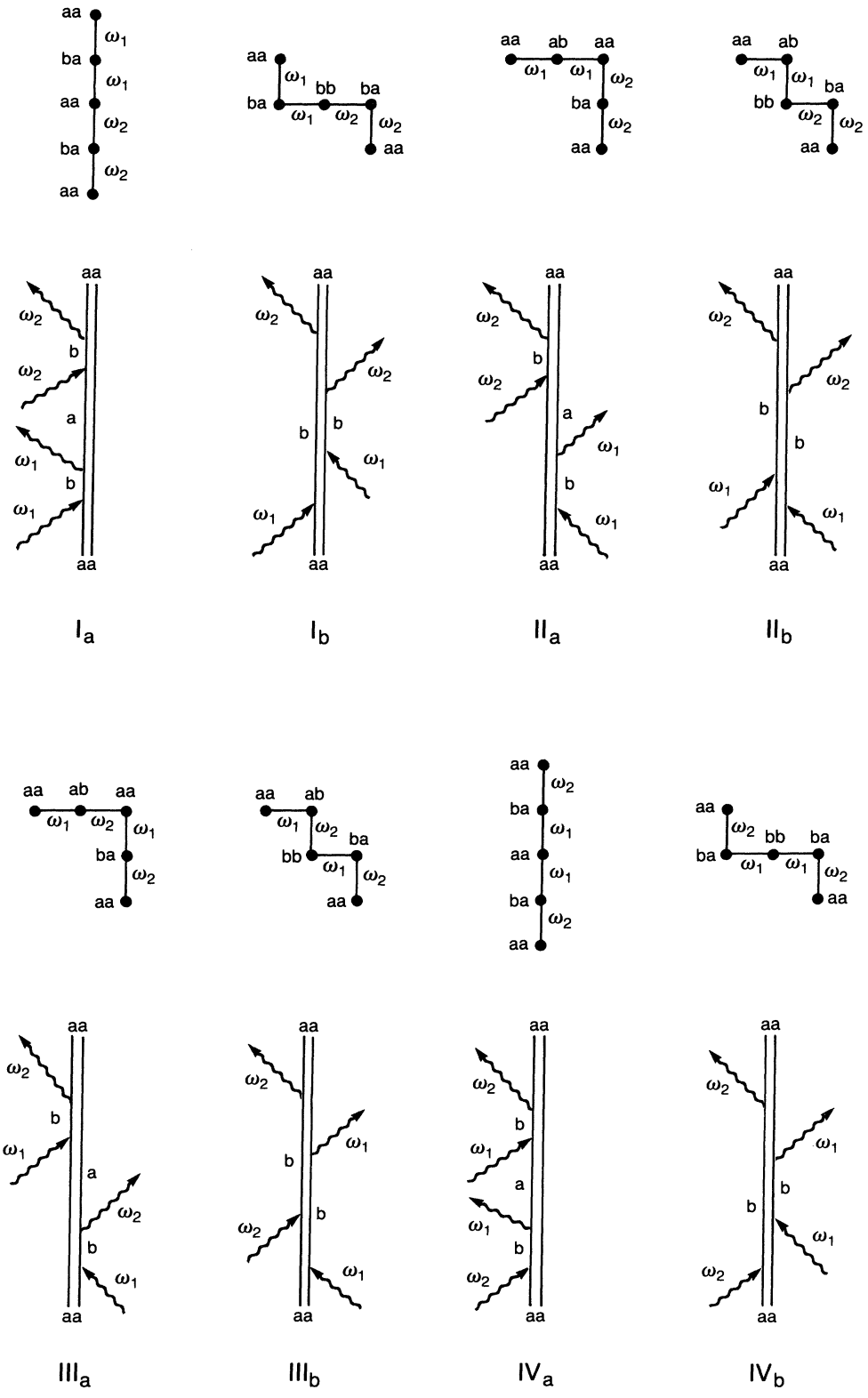

FIG. 7. The eight pathways leading to the eight terms of Eq. (42) describing a system with the relaxation scheme shown in Fig. 3(b). For comparison with the work of other authors (Refs. 10 and 11), the corresponding double-sided Feynman diagram is shown below each pathway. The Feynman diagrams follow the convention that the time axis points vertically upward.

fere (i.e., the first E_2 interaction occurs *before* the second E_1 interaction). The contributions of these pathways cannot be viewed as a preparation by E_1 followed by detection by E_2, and hence are absent in the expression of the sequential model. Their significance is obvious, however, by inspection of Fig. 7. Let us consider, for example, diagram IV$_a$. The first interaction gives rise to a dipole moment oscillating at frequency ω_2, and the second interaction then produces a contribution to ρ_{aa} oscillating at the beat frequency $\omega_1-\omega_2$. The third interaction, involving the ω_1 field, then produces a dipole moment oscillating a frequency ω_2, which thus contributes to the absorption of the ω_2 field. This contribution is significant only if the population can response to the beat frequency between the input waves, which occurs only if $(\omega_2-\omega_1)/(\gamma_b+\gamma_a)<1$. Consequently, the width associated with this contribution (i.e., tuning ω_2 with ω_1 held fixed) is $\sim(\gamma_b+\gamma_a)$.

In conclusion, we summarize the main results of this paper. (1) We have derived an expression [Eq. (20)] for the $\chi^{(3)}$ susceptibility for a two-level system that generalizes previous treatments, (a) by including a more realistic T_1 relaxation mechanism [Fig. 3(a)] and (b) by applying to nonimpact line shapes.[8] (2) By applying this expression to pump-probe experiments, we have derived an expression for the probe absorption line shape [Eq. (35)] that is in contradiction to the conventional expression obtained using the sequential model. This difference manifests itself as a dip in the probe absorption profile at the pump-laser frequency even in a homogeneously broadened system.[2–4,15,16] (3) We have traced the origin of this discrepancy to interference effects between the two fields which are ignored if we allow the E_2 field to probe the system as prepared only by the E_1 field. The $\chi^{(3)}$ formalism automatically incorporates these interference effects properly.

ACKNOWLEDGMENTS

The authors wish to thank M. G. Raymer, Y. R. Shen, and C. R. Stroud for useful discussions. We gratefully acknowledge the support of the National Science Foundation and S.M. gratefully acknowledges the support of an Alfred P. Sloan Foundation grant.

[1]A. Yariv, *Quantum Electronics,* 2nd ed. (Wiley, New York, 1975), Sec. 8.7, and particularly Eqs. (8.7)—(8.17) on p. 171; M. Sargent III, M. O. Scully, and W. E. Lamb, Jr., *Laser Physics* (Addison-Wesley, Reading, Mass., 1974), Sec. 10-1 and in particular Eq. (27) on p. 151.

[2]S. E. Schwartz and T. Y. Tan, Appl. Phys. Lett. 10, 4 (1967).

[3]V. S. Letokhov and V. P. Chebotayev, *Nonlinear Laser Spectroscopy* (Springer, Berlin, 1977); M. Sargent III, Phys. Rep. 43, 223 (1978).

[4]R. W. Boyd, M. G. Raymer, P. Narum, and D. J. Harter, Phys. Rev. A 24, 411 (1981).

[5]L. W. Hillman, R. W. Boyd, J. Krasinski, and C. R. Stroud, Jr., Opt. Commun. 45, 416 (1983).

[6]N. Bloembergen, *Nonlinear Optics* (Benjamin, New York, 1965).

[7]N. Bloembergen, H. Lotem, and R. T. Lynch, Jr., Indian J. Pure Appl. Phys. 16, 151 (1978).

[8]S. Mukamel, Phys. Rep. 93, 1 (1982).

[9]S. Mukamel 28, 3480 (1983).

[10]T. K. Yee and T. K. Gustafson, Phys. Rev. A 18, 1597 (1978).

[11]S. A. Druet and J. P. E. Taran, Prog. Quant. Electron. 7, 1 (1981).

[12]V. Mizrahi, Y. Prior, and S. Mukamel, Opt. Lett. 8, 145 (1983).

[13]See, e.g., I. Oppenheim, K. E. Shuler, and G. H. Weis, Adv. Mol. Relaxation Processes 1, 13 (1967).

[14]S. Mukamel, D. Grimbert, and Y. Rabin, Phys. Rev. A 26, 341 (1982).

[15]B. R. Mollow, Phys. Rev. A 5, 2217 (1972).

[16]S. Haroche and F. Hartmann, Phys. Rev. A 6, 1280 (1972).